High-velocity impact of plates

M. Alves, G. B. Micheli and L. Driemeier

Group of Solid Mechanics and Structural Impact — GMSIE
Department of Mechatronics and Mechanical Systems Engineering – University of São Paulo – São Paulo – 05508-900 – Brazil

Abstract

This work explores the failure of plates due to the impact of hard spheres traveling at high speed. The tests were run in a specially designed gas-gun capable of launching projectiles at a speed of up to 160m/s. A series quasit-static and dynamic compression material tests were performed in order to obtain the major material parameters. The analysis was performed in a comercial finite element code and two failure criteria were used. A continuum damage mechanics failure model predicted reasonably well the ballistic limit for the plate under analysis.

Key words: failure, impact, damage, dynamic compression test, plate perfuration.

1 Introduction

The analysis of structures under severe dynamic loads, as the high velocity impact of a hard sphere against a plate may look simple. A closer investigation of this problem, however, will at once reveal to the engineer that quite a few unexpected issues should be addressed before a detailed analysis is carried on.

A first question would be whether a theoretical analysis suffices for the problem at hand. In this case, the engineer should have some basic knowledge on plastic analysis of structures, a topic not frequently taught in undergraduation courses. If the analysis is based on finite elements, a reliable programme capable of large strains dynamic analysis should be used. In the brazilian context, such a software is not readily available, suggesting that the problem can only be solved with imported technology.

Moreover, it will be necessary to know the material properties with certain detail and, again in the brazilian context, this task is far from being common

[1] Corresponding author: M. Alves, e-mail: maralves@usp.br

(a) (b)

Fig. 1. (a) Overview of the projectile launcher. (b) Protection chamber for the tests.

when considering that it may be necessary to perform dynamic tests, whereby the material is pulled or compressed at high velocity in order to reveal its strength. It is also worth to comment that, if material failure is to be analysed, then it is necessary to choose a failure criterion, such that the whole procedure of this apparently simple analysis is somewhat difficult to go through entirely.

The aim of this article is to show how a high-velocity impact problem was approached and solved by the authors. We start first by describing in section 2 the experimental apparatus to perform the ballistic tests. In section 3 the procedure for dynamic material characterisation is outlined, together with the major material properties as described by constants which fit some constitutive laws. Section 4 gives an overview on the failure criterion which performed best for the present problem. The finite element analysis is detailed in section 5, with section 6 discussing the results.

2 Experimental apparatus and results

The plate impact tests reported here were all performed in the projectile launcher, also called gas-gun, shown in Figure 1.

In order to set the right pressure for a test, a series of pressure *versus* velocity shots was carried out and the resulting calibration curve was used in the various impact tests, Figure 2(a). The velocity was always accurately measured with an infra-red detector, Figure 2(b), installed in the exit of the gas-gun barrel.

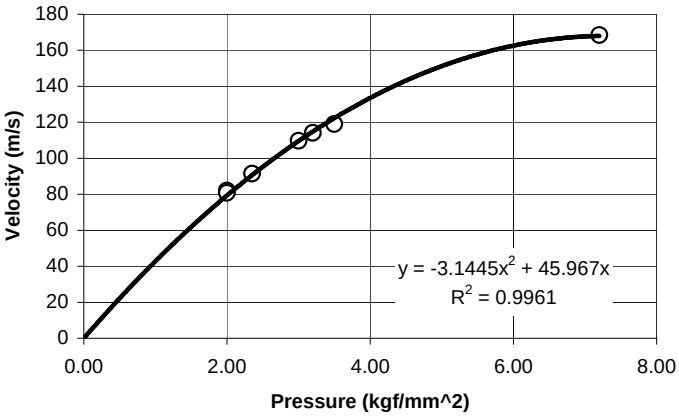

(a)

(b)

Fig. 2. (a) Pressure *versus* velocity for the gas gun with bore diameter of 50mm. (b) Infra-red velocimeter.

A typical test arrangement consists of fixing a sheet of metal in the anvil and firing against it the projectile. The sheets are from a large as delivered aluminium sheet cut in squares of 350mm $\times$ 350mm $\times$ 1.6mm with 8$\times$ 20mm holes for clamping around the edges via a steel ring such that the structural model consists of a clamped circular plate of diameter 350mm. The plates were impacted with a hard steel sphere of diameter and mass of 20 mm and 33 grammes, respectively. The various impact tests aim at detecting a threshold velocity which just caused material failure. The actual detection of the material failure was done visually. There are many issues behind this crude detection of material failure but this simple method gives an undisputable indication of failure. Also, in the FE analysis, the smallest finite element had dimensions compatible with a naked eye detection of failure.

It is clear from Figure 3 that the impact velocity which causes material failure is within the narrow range of 116.03 m/s and 119.02 m/s, with an average impact velocity of 117.16 m/s. Total perforation occurred at an impact velocity of 121.44m/s.

Figure 4 shows details of the failure pattern that occurs in the plate at various impact velocities. In figure (a) the impact velocity is 116.03 m/s and failure was by tearing. Increasing a little bit the impact velocity to 119.02 m/s one has another mode of failure, Figure 4(b). The failure is a classical example of pettaling, where tearing is followed by significant bending of the cracked pieces. It is interesting to note in this impact event the more or less symmetrical failure. Another mode of failure is by shear plugging, Figure 4(c), impact velocity of 117.37 m/s. Total pettaling perfuration occurs for high impact velocities, as in Figure 4(d) for $V_0 = 136.17$m/s.

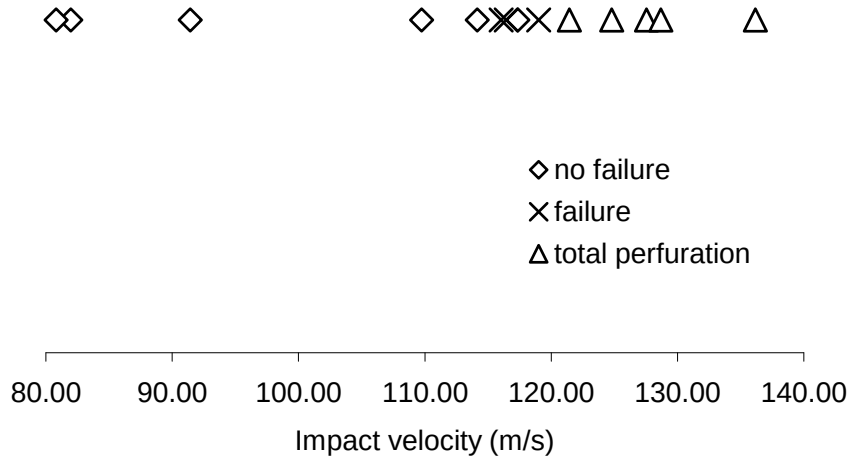

Fig. 3. Plate response to the impact velocity.

(a) (b) (c) (d)

Fig. 4. Plate hit by a hard sphere at impact velocities of (a) $V_0 = 116.03$m/s, (b) $V_0 = 119.02$m/s, (c) $V_0 = 117.37$m/s and (d) $V_0 = 136.17$ m/s.

3 Material characterisation

In order to analyse the impact event described in the previous section, it is necessary to measure the properties of the material the plate is made. This proves to be an illusory task if we consider that the impact event causes extremely rapid changes in the strains. These high strain rates may affect the material strength so its properties need to be determined under such extreme conditions.

A more common task is the measurement of quasi-static material stress–strain curve, shown in Figure 5 for the aluminium plate. From the measured data it is possible to obtain the material parameters which best fit the non-linear hardening law

$$\sigma_0 = (A + B\varepsilon^{p^n}), \tag{1}$$

where no damage or thermal effects are considered, with $A = 320.4$MPa, $B = 675.0$MPa and $n = 0.7624$ being material input constants and ε^p the effective plastic strain. Also, for this material, the elastic modulus is $E = 72739$MPa and the strain to failure was measured to be $\varepsilon_{fa} = 0.10$.

Observe that some of the curves in Figure 5 show loading cycles being applied

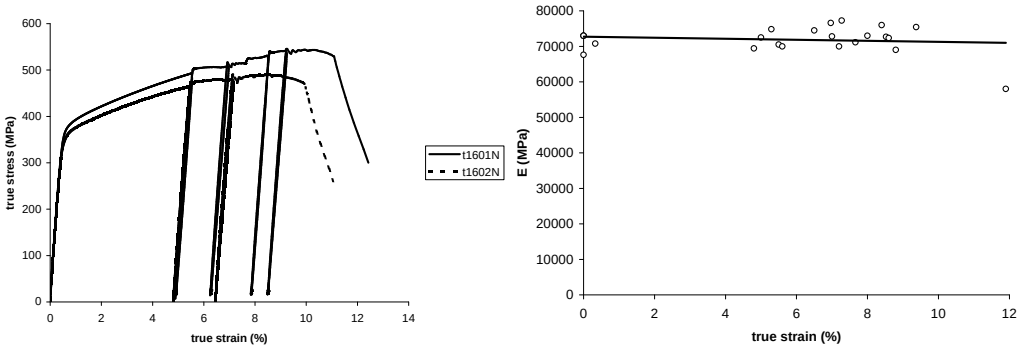

Fig. 5. (a) Unidimensional true stress–strain curve for the aluminium alloy. (b) Elastic modulus degradation under tensile loading.

Fig. 6. Hopkinson bar in GMSIE.

to the specimens. The material response to these cycles can be used to infer parameters necessary for a damage model to be commented later, like the degradation of the elastic modulus in Figure 5(b).

The experimental procedure for dynamic material characterisation was based on the Split Hopkinson pressure bar (SHPB) shown in Figure 6. Details of how the dynamic curves shown in Figure 7 were obtained can be found elsewhere [1, 2].

The material stress–strain behaviour at different strain rates measured in the SHPB are shown in Figure 7. From these curves, it is possible to compute the parameters for the Cowper–Symonds equation

$$\sigma_d = \sigma_s \left\{ 1 + \left(\frac{\dot{\varepsilon}}{C} \right)^{1/q} \right\}, \tag{2}$$

which describes the material strain rate hardening [3, 4]. The various dynamic

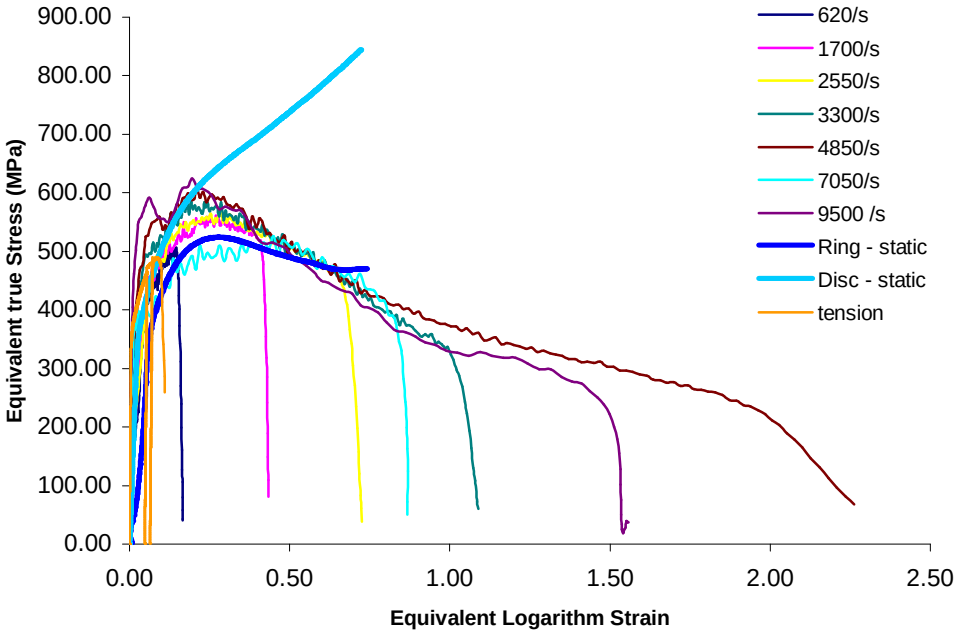

Fig. 7. Stress–strain behaviour at various strain rates and room temperature.

Q_1 (MPa)	Q_2 (MPa)	C_1	C_2	ε_D	S	$D_{c_{num}}$	$D_{c_{exp}}$
80	220	80	5	0.05	3.3	0.19	0.19

Table 1
The CDM parameters.

tests yield $C = 2.220E5$ s^{-1} and $q = 2.391$.

As for the parameters of the continuum damage mechanics, CDM, model they were measured in the tensile tests [5,6] but in the present case we cross-checked the results by simulating the tests in LS-DYNA with Material Type 103 and guessing the CDM material parameters so to obtain a good match between the experimental and numerical load–displacement curve. It turns out that the various CDM material constants in the constitutive equation available in LS-DYNA

$$\sigma = \sigma_0 + Q_1[1 - \exp(-C_1\varepsilon^p_{eq}] + Q_2[1 - \exp(-C_2\varepsilon^p_{eq}] + \left(\frac{\dot{\varepsilon}^p}{C}\right)^{1/q}, \qquad (3)$$

are the ones listed in Table 1, with C and q being the Cowper–Symonds constants already given.

4 Failure criteria

Failure of materials is an important issue, with many open questions in the literature. The problem becomes even more troublesome in the present exper-

imental programme if one considers that falure occurs under severe dynamic loads. We opt in this article to report results using two relatively simple failure criterion, both available in LS-DYNA [7].

The first one states that failure occurs when the equivalent strain in a finite element reaches the value of ε_{fa}. When this happens, LS-DYNA erodes the element so it loses its ability to sustain load. This criterion is known to be very poor but being so popular we found interesting to explore.

The other criterion is based on continuum damage mechanics, as anticipated when giving the relevant material parameters. The model theory is given elsewhere [8] and we quote that damage evolution starts when $\varepsilon_{eq} > \varepsilon_D$ according to

$$\dot{D} = \frac{\sigma_{eq}^2 R_\nu}{2E\bar{S}}\dot{\varepsilon}_{eq}, \tag{4}$$

where ε_{eq} and σ_{eq} are the equivalent strain and stress, $\bar{S}$ is a material constant and

$$R_\nu = \frac{2}{3}(1+\nu) + 3(1-2\nu)\left(\frac{\sigma_h}{\sigma_{eq}}\right)^2, \tag{5}$$

ν being the Poisson ratio and σ_h the hydrostatic stress.

The criterion works similary as the failure strain but the finite element is eliminated from the mesh when the critical damage, D_c is reached.

5 Finite element analysis

It is evident that the mesh could play an important factor on the determination of the ballistic limit and failure modes of the impacted plates.

We monitored the processing time and checked whether there would be total perfuration. Using an impact velocity variation of 2.5 m/s, we determined the so called ballistic limit. We simply defined it as the threshold velocity for which the plate was perfurated by the sphere, allowing it to pass through. This limit proved to be mesh dependent, as can be seen in Figure 8.

However, the increase of the number of elements in the impact region did not affect much the ballistic velocity. If we were to use a high density mesh, the processing time would be far too long so we prefered to maintain a balance between these two factors. These remarks are valid for both shell and solid finite elements used here, with the final meshes depicted in Figure 9.

We tested six different shell finite element formulations. Only two elements perform well in terms of the expected failure pattern and we opt for the Belytschko-Leviathan finite element for the cases when the plates are modelled

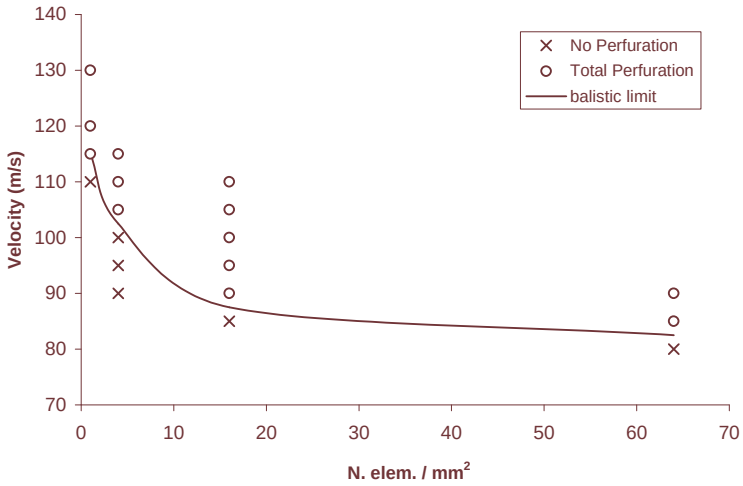

Fig. 8. Influence of the mesh density on the ballisitic limit.

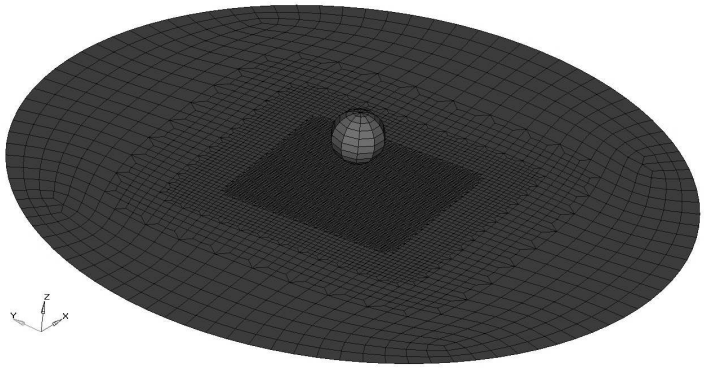

Fig. 9. Final finite shell element mesh used in the analysis. The solid element mesh was extruded from this one.

with shell elements. It is known that these Belytschko-Leviathan elements are embodied with an hourglass control feature allowing them to reproduce bending and twisting deformation.

Damping was chosen based on measurements of the vibration of the plate when fit in the rig. The measurements were performed with no contact by a laser Doppler. Also, we run many analysis with different friction coefficients and found that the higher the friction the smaller the after perfuration sphere velocity. This, together with information from the literature [9], suggested a friction coefficient of 0.02 in all the analysis.

The integration order is another parameter that can be set in LS-DYNA input file. It is represented by numbers from 0 to 5. From the runs we made, it transpired that integration order 3 was better because the failure pattern revealed to be more symmetric. As for the hour-glass control, we run all the five cases values in LS-DYNA, concluding that the crack pattern associated with number 5 gives a more physically consistent result.

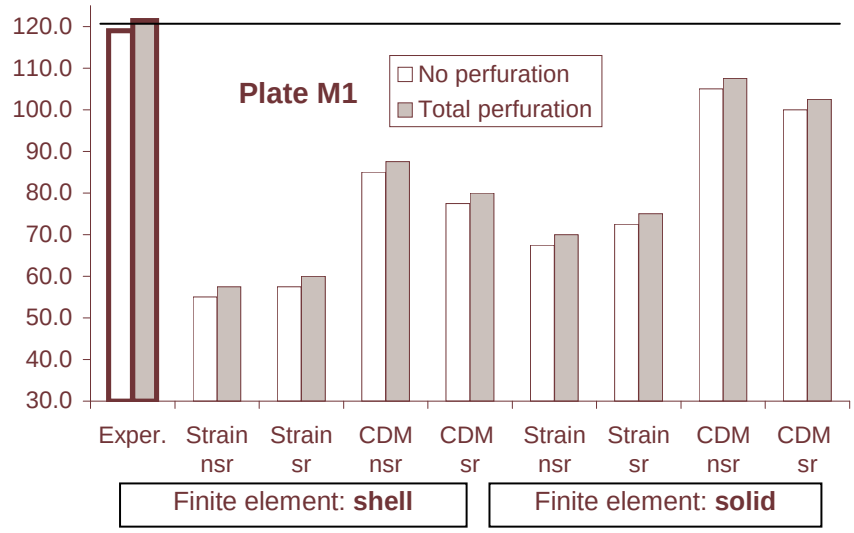

Fig. 10. Ballistic limit for the aluminium plate according to the failure criteria. (nsr), sr – (non)-strain-rate sensitive, respectively.

6 Discussion

We have now all the setting for the analysis of the impact of the hard steel sphere against the aluminium plates. Ranging from material parameters, mesh, LS-DYNA input parameters and experimental information like the impact point and velocity, all these data can now be put on a single perspective, as shown in Figure 10.

The experimental ballistic limit for this plate is 121.4 m/s. Figure 10 reveals that the analysis using shell elements yields poor results, regardless of the failure model used. It is also evident from the figure that the failure strain failure model predicts a ballistic limit with an error between 60% and 110%, according to the finite element type and the consideration or not of the strain rate in the analysis.

It is clear from Figure 10 that the solid finite element is more appropriate for this type of investigation. Also, the CDM model performs better than the failure strain criterion. Indeed, the predictions for the ballistic limit is within an error of 13% and 52%, again according to the finite element type and the consideration or not of the strain rate in the analysis.

It is interesting to observe that the non-strain rate sensitive model run with the solid element gives the best performance. This cannot be explained easily but we point to the fact that it is not known from the experimental programme the damage model parametes under dynamic conditions.

7 Conclusions

This article reports on a set of experiments dealing with the high velocity impact of hard objects onto plates. The tests were performed in a specially designed projectile launcher. The material parameters were measured under static and dynamic conditions. The analysis was explored as far as the type of element is concerned, together with parameters like friction, hour glass control, integration points, etc...

It is clear from the results that it is difficult to predict the threshold velocity which causes total penetration of the hard projectile. Even so, the present study clearly shows that the use of the failure strain as a failure criterion leads to huge errors.

On the other hand, the continuum damage mechanics models is quite reasonable when considering the not so large errors and the relative easiness the parameters can be obtained.

Finally, it is indicated that the experimental programme is somewhat complex but possible to be performed in Brazil. On the other hand, we are still rather dependent of imported technology for the analysis since no finite element code for structural impact problems is readily available in Brazil. Hence, Figure 11, which shows a comparison among experimental fracture, shell and solid finite element model, is still a chalenge for our technical community to obtain.

References

[1] F. Galina, R. S. Birch, and M. Alves. Design of a split hopkinson pressure bar. In *Brazilian Conference on Mechanical Engineering*, 2003.

[2] M. Alves and N. Jones. *Impact Loading of Lightweight Structures*. W.I.T. Press, 2005.

[3] M. Alves. A strain rate dependent material constitutive law valid for large strains. *Journal of Engineering Mechanics - ASCE*, 126:215–218, 1999.

[4] M. Alves. Prediction of the dynamic flow stress. *Structural Engineering and Mechanics*, 20:495–504, 2005.

[5] M. Alves, J.L. Yu, and N. Jones. Elastic modulus degradation in continuum damage mechanics. *Computers & Structures*, 76(6):703–712, 2000.

[6] M. Alves. Measurement of ductile material damage. *Journal of Mechanics of Structures and Machines*, 29(4):451–476, 2001.

[7] LS-DYNA. *Theorethical manual*. Livermore Software, 1998.

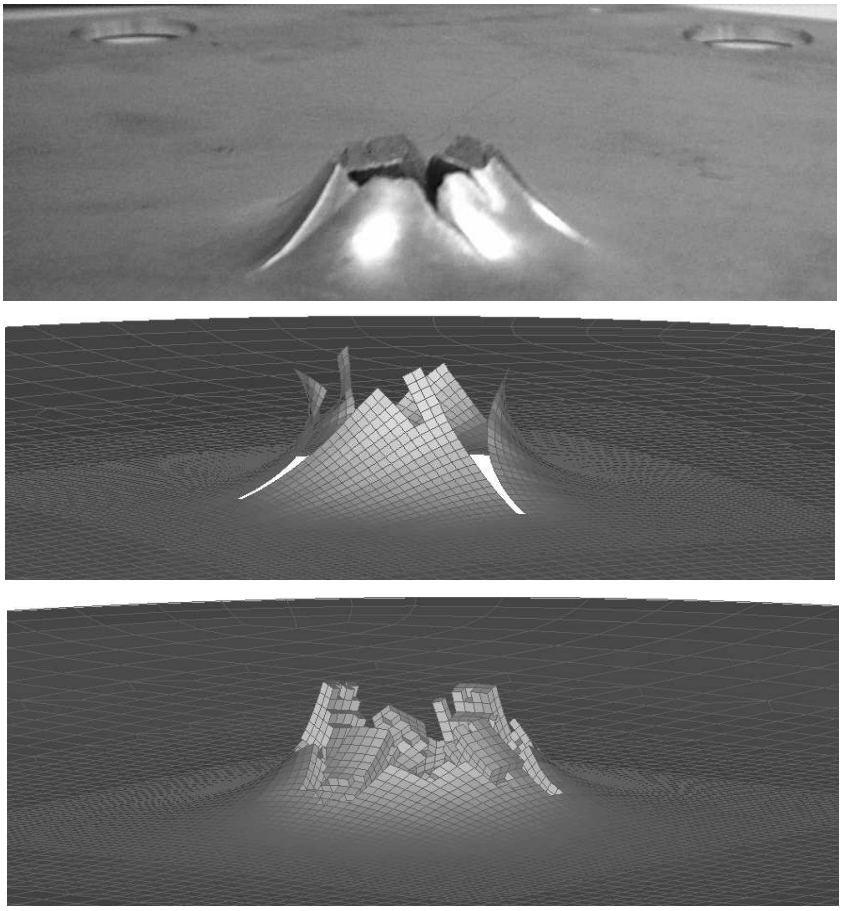

Fig. 11. Fracture in an impacted plate and a shell plus solid finite element model.

[8] J. Lemaitre. *A Course on Damage Mechanics*. Springer–Verlag, Berlin, 1992.

[9] T. Borvik, A.H. Clausen, M. Eriksson, T. Berstad, O. S. Hopperstad, and M. Langseth. Experimental and numerical study on the perforation of AA6005-T6 panels. *International Journal of Impact Engineering*, 32:35–64, 2005.